MADPH-01-1230
WM-01-107
hep-ph/0106277
June, 2001

Search for $t \to ch$ at e^+e^- Linear Colliders

Tao Han* and Jing Jiang†
Department of Physics, University of Wisconsin,
1150 University Avenue, Madison, WI 53706, USA

Marc Sher‡
Nuclear and Particle Theory Group, Physics Department,
College of William and Mary, Williamsburg, VA 23187, USA

Abstract

We study the rare top-quark decay $t \to ch$, where h is a generic Higgs boson, at a linear collider. If kinematically accessible, all models contain this decay at some level due to quark flavor mixing. Some models, such as Model III of the two-Higgs doublet model, have a tree-level top-charm-Higgs coupling, and the branching ratio is close to 0.5%. Others, such as the MSSM, have a coupling induced at one-loop, and can have a branching ratio in the range of $10^{-5} - 5 \times 10^{-4}$. We find that a linear collider of $\sqrt{s} = 500$ GeV and a luminosity of 500 fb^{-1} will begin to be sensitive to this range of the coupling.

PACS numbers: 12.60.Fr, 14.80.Cp, 14.65.Ha, 12.15.Mm

*than@pheno.physics.wisc.edu

†jiang@pheno.physics.wisc.edu

‡sher@physics.wm.edu

I. INTRODUCTION

Two of the most important unanswered puzzles of elementary particle physics are the nature of electroweak symmetry breaking and the origin of flavor. Both are implemented in the Standard Model of particle physics in an *ad hoc* manner. Often, extensions of the Standard Model (SM) treat these two problems separately; extended Higgs models do not address the flavor problem and flavor symmetry models do not substantively address the nature of electroweak symmetry breaking. Yet, there are no dynamical models satisfactorily addressing the two puzzles coherently. Since the top quark is so heavy, with a mass on the order of the electroweak symmetry breaking scale, it is tempting to consider the possible special role of the top quark in the electroweak symmetry breaking sector and in the quark flavor sector, and its interactions could shed light on both problems. Flavor-changing-neutral-current (FCNC) decays of the top quark [1] could be very sensitive to various extensions of the Standard Model that address both of these puzzles.

Most studies of flavor-changing-neutral-current top-quark decays have examined the decay of the top quark into a charmed quark and a gauge boson [2] (either a gluon, photon or a Z). However, the flavor-changing-neutral-current decay most likely to shed light on the nature of electroweak symmetry breaking is the decay of the top quark into a charmed quark and a Higgs boson [1,3] (or the decay of the Higgs boson into a top and a charmed quark if kinematically preferred). It is this interaction that we study in this paper.

All models will contain a top-charm-Higgs (TCH) vertex at some level[1]. Even in the Standard Model, a one-loop diagram gives a contribution, but it is GIM-suppressed and extremely small [3]. In extensions of the Standard Model, however, such a vertex can occur either at tree level or at a non-GIM-suppressed one-loop level.

One of the simplest extensions of the Standard Model has a tree-level TCH vertex. This is the general two-Higgs doublet model, referred to as Model III, in which no discrete symmetries are imposed to avoid flavor-changing neutral currents. In this case, the quark Yukawa coupling matrices consist of two parts, $y = y_1 + y_2$, where y_i is the coupling to the i'th Higgs doublet. Since diagonalizing y will not, in general, diagonalize y_1 and y_2, there will be tree-level flavor-changing neutral currents. Cheng and Sher [4] noted that if one wishes to avoid fine-tuning, then the observed structure of the mass and mixing hierarchy suggests that the FCNC vertex $\xi_{ij}\ \bar{q}_i q_j h$ is given by the geometric mean of the Yukawa couplings of the quark fields[2]

---

[1]Whether a TCH vertex exists does, in part, depend on nomenclature. Strictly speaking, one should consider the "Higgs" to be the other member of the isodoublet containing the longitudinal components of the weak vector bosons; after all, it is this field that is associated with spontaneous symmetry breaking. With that definition, the Yukawa couplings are necessarily flavor-diagonal. Here, we use the word "Higgs" to indicate a scalar field whose mass eigenstates contain some part of the field associated with spontaneous symmetry breaking.

[2]We note that some authors may have used a different normalization for λ_{ij} by a factor of $\sqrt{2}$ larger than ours. Since the ansatz is order of magnitude only, either definition is acceptable.

$$\xi_{ij} = \lambda_{ij} \frac{\sqrt{m_i m_j}}{v} \ , \tag{1}$$

where $v = 246$ GeV is the weak scale, and the λ_{ij} are naturally all of $\mathcal{O}(1)$. This ansatz has no conflict with current phenomenological observation, and yet predicts rich physics in the heavy-flavor generations. Under this ansatz, the top-charm-scalar coupling ξ_{ct} is the biggest in the model, and is approximately 0.05.

Model III is fairly general. A number of more specific models have a large TCH coupling as well. Burdman [5] studied a topcolor model [6], which gave a large TCH coupling of the same order as Model III (although his "Higgs" boson had a mass larger than that of the top quark). A topflavor model [7] analyzed the flavor-changing coupling of the top and charm to a top-pion, finding a TCH coupling that is substantially larger than that of Model III. Recently, a bosonic topcolor model [8] was proposed that automatically has the TCH coupling as the *largest* fermionic coupling of the Higgs boson. An extensive analysis of models with additional singlet quarks (Q) by Higuchi and Yamamoto [9] gives a flavor-changing coupling which is proportional to the product of the cQ and tQ mixings; this can be larger than the Model III coupling. In general, in models which treat the top quark differently than other quarks motivated by its weak-scale mass, one might expect TCH coupling of Model III size or larger.

There have been numerous studies of Model III with the above ansatz, examining K, B, μ and τ decays, as well as K^0, B^0 and D^0 mixing [10]. Here, however, we will be concerned with the large TCH coupling only.

The rate for the decay $t \to ch$ was first calculated by Hou [11]. For a top-quark mass of 175 GeV, the branching ratio of $t \to ch$ to $t \to bW^+$ is

$$\begin{aligned} \frac{\Gamma(t \to ch)}{\Gamma(t \to bW^+)} &\approx \lambda_{ct}^2 \ \frac{m_c}{m_t} \ \frac{(1 - \frac{m_h^2}{m_t^2})^2}{(1 - \frac{m_W^2}{m_t^2})\,(1 - \frac{m_W^2}{m_t^2} - 2\,\frac{m_W^4}{m_t^4})} \\ &\approx 0.009 \ \lambda_{ct}^2 \ \left(1 - \frac{m_h^2}{m_t^2}\right)^2 . \end{aligned} \tag{2}$$

This implies that the branching fraction of $t \to ch$ can be typically of 10^{-3} or higher for $\lambda_{ct} \sim \mathcal{O}(1)$. If the Higgs is heavier than the top, one can have $h \to \bar{t}c + \bar{c}t$, as first discussed in Ref. [11]. This leads to the process $e^+e^- \to h^0 A^0 \to \bar{t}\bar{t}cc + \bar{c}\bar{c}tt$ at a linear collider [12], to like-sign top-pair production at the LHC [13], and to the linear collider process $e^+e^- \to \bar{\nu}_e \nu_e (\bar{t}c + \bar{c}t)$ [14]. These processes all assume a Higgs boson heavier than the top, however, and recent electroweak precision data [15], as well as hints from LEP [16], prefer the scenario of a rather light Higgs boson, making $t \to ch$ kinematically accessible. As one can see from Eq. (2), the branching ratio for $\lambda_{ct} = 1$ and a 115 GeV Higgs mass is 3×10^{-3}.

If one looks at one-loop processes, there are many more possibilities. Most extensions of the Standard Model will avoid the GIM suppression that makes the coupling so small in the

---

Similarly, we have not worried about the running mass effects at different renormalization scales, and we simply take the pole masses for m_t and m_c for our analysis.

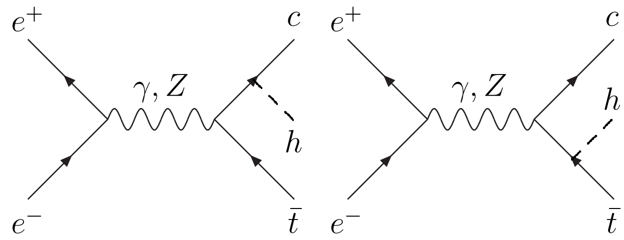

FIG. 1. Tree level Feymann diagrams for $e^+e^- \to \bar{t}ch$ process. Diagrams for $e^+e^- \to t\bar{c}h$ process are similar.

Standard Model [3]. The most popular extension is the MSSM. In this model, there *must* be a Higgs boson lighter than the top quark, and so the decay will occur. An extensive analysis of $t \to cH$, where H refers to any one of the three neutral scalars in the MSSM, was carried out in Ref. [17]. They show that the dominant contribution comes about from loops with gluinos and squarks, and the branching ratio ranges from 10^{-5} to 5×10^{-4} over the MSSM parameter space. In an R-parity violating SUSY model, a one-loop contribution can also give [18] a branching ratio as large as 10^{-5}.

We see that models with a tree-level TCH coupling have branching ratios of the order of $10^{-3} - 10^{-2}$, and models with a one-loop coupling can have branching ratios of the order of $10^{-5} - 10^{-4}$. What level is experimentally detectable at high energy colliders? Recently, discovery limits at the LHC were calculated [20] and are approximately 5×10^{-5}. While the results are quite encouraging, detailed Monte Carlo simulation would be needed to draw a definitive conclusion due to the complicated background issue at hadron colliders. In a linear collider, backgrounds are much more manageable, although signal cross sections are lower. In this paper, we assume that a light Higgs boson will be observed and examine in detail the discovery potential for its FCNC coupling at a linear collider.

II. TOP-CHARM-HIGGS COUPLING AT A LINEAR COLLIDER

A. Production Cross Section

Using the coupling constant given in Eq. (1), we wish to explore the limits obtainable on λ_{ct} at a linear collider. We consider the process

$$e^+e^- \to \bar{t}ch,\ t\bar{c}h\ , \tag{3}$$

where the corresponding Feynman diagrams are shown in Fig. 1. The dominant contribution to process (3) is from $e^+e^- \to t\bar{t}$ followed by $t\,(\bar{t})$ decay into $ch\,(\bar{c}h)$, namely $\sigma(e^+e^- \to t\bar{t}) \times [Br(t \to ch) + Br(\bar{t} \to \bar{c}h)]$. The decay branching ratio is calculated and shown in Fig. 2(a), where we see that for $m_h = 120$ GeV and $\lambda_{ct} = 1$, $t \to ch$ has a branching ratio of 2.8×10^{-3}. At tree level, top-pair production has a total cross section of 580 fb at the center-of-mass energy $\sqrt{s} = 500$ GeV. Thus each channel will have a cross section of 1.6 fb. The total cross section of $e^+e^- \to \bar{t}ch$ and $t\bar{c}h$ is presented in Fig. 2(b) as a function of

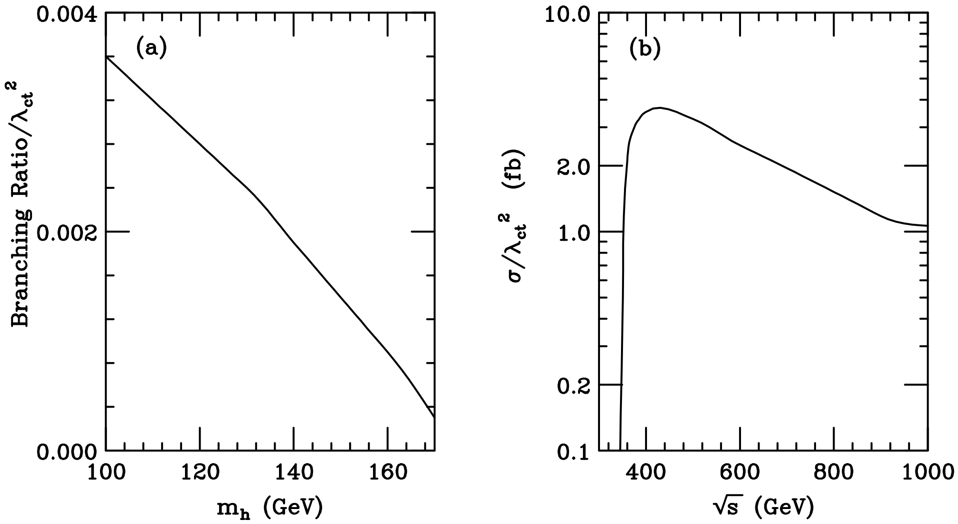

FIG. 2. (a) Branching ratio of $t \to ch$ decay as a function of m_h and (b) Cross section for $t\bar{c}h + \bar{t}ch$ production as a function of center-of-mass energy in e^+e^- collisions for $m_h = 120$ GeV.

$\sqrt{s}$, where and henceforth $m_h = 120$ GeV is chosen for illustration. The total cross section scales as λ_{ct}^2 and is of order of 1 fb for $\lambda_{ct} = 1$.

B. Signal And Background

Since we are motivated to consider a light Higgs boson with a mass around 120 GeV, we concentrate on the process in which the Higgs boson decays to $b\bar{b}$ and t decays into bW. The W can then undergo either hadronic (2 jets) or leptonic ($\ell^\pm\nu$) decays. The $h \to b\bar{b}$ branching ratio for $m_h = 120$ GeV is about 85%. The signal thus consists of the following channels in the final state

$$e^+e^- \to b\bar{b},\, b + 3\, jets \qquad (4)$$

$$\text{or} \quad \to b\bar{b},\, b\,\ell^\pm\nu + 1\, jets. \qquad (5)$$

The primary background to the above signal is from the SM top-pair production $e^+e^- \to t\bar{t} \to \bar{b}W^+bW^-$, with one W decaying hadronically and the other decaying either hadronically or leptonically, depending on which signal of Eqs. (4) and (5) we are looking at. In order to identify the signal from the background, we require that 3 b's be tagged. The efficiency for a single b tagging is taken to be 65% [19]. This still does not eliminate the background: For the case that both W's decay hadronically, one out of the four non-b jets from W decay to light quarks may be misidentified as a b-jet. We assume the misidentification to be 1% for each jet. Thus for four jets the total misidentification probability is 4%. Similarly, for the case that one of the two W's decays leptonically, one of the two non-b jets from W decay to light quarks is misidentified as a b-jet. The SM background induced by one W decay into $\bar{c}b$ is negligible due to the small size of the CKM mixing matrix element $V_{cb} \sim 0.04$. The entries of the first row in Table I show the signal and background cross sections at $\sqrt{s} = 500$ GeV before applying any kinematical cuts but

	signal	bg(hadronic)	bg(leptonic)	bg(total)
no cuts	0.75	6.56	3.23	9.79
basic cuts	0.60	0.28	0.26	0.54
addi. cuts	0.52	0.13	0.12	0.25

TABLE I. Cross sections in fb at $\sqrt{s} = 500$ GeV for signal ($m_h = 120$ GeV and $\lambda_{ct} = 1$) and hadronic, leptonic and total backgrounds before and after cuts.

including decay branching fractions and b-tagging efficiencies. We find that the background rate is still overwhelming.

We next try to make use of the distinctive signal kinematics by reconstructing h, t, $\bar{t}$ and W masses from the final state momenta. To simulate the detector response, we smear the jet energies according to a Gaussian spread

$$\frac{\Delta E}{E} = \frac{45\%}{\sqrt{E}} \oplus 2\% \ , \tag{6}$$

where $\oplus$ denotes a sum in quadrature. For the signal, we first consider the case where W decays into two jets. Of the three tagged b's, we choose two b's whose invariant mass is closest to m_h and identify them as the b's coming from h decay (M_h^{rec}). Then from the three light jets we pick the jet that, together with $b\bar{b}$ selected above, produces an invariant mass (M_t^{rec}) that is closest to m_t. This jet is now identified as c from $t \to cb\bar{b}$ decay. The remaining two jets can be used to construct the W mass M_W^{rec} and with the third b, we have $M_{\bar{t}}^{rec}$. If W decays into $l\nu$, it is simpler. We simply need to choose two of the three b-jets to construct M_h^{rec}. The only non-b jet is identified as c. We get M_W^{rec} from the momenta of $\ell^\pm$ and missing energy assigned to ν, after adding the momentum of the third b, we have $M_{\bar{t}}^{rec}$. For the background in which W decays hadronically, we randomly pick one from the 4 non-b jets and assume it to be misidentified as a b-jet. Then we follow the same construction as for the signals, we will get M_h^{rec}, M_t^{rec}, $M_{\bar{t}}^{rec}$ and M_W^{rec}. For the background when W decays leptonically, we randomly choose one of the two non-b jets to be misidentified as b and again follow the analysis for the signals to get the four reconstructed invariant masses. The normalized differential distribution with respect to these reconstructed masses are shown in Fig. 3 for signals and backgrounds. The characteristic difference between the signal and background is evident from these mass distributions. The first crucial reconstructed mass is M_h^{rec}. A peak structure in this variable provides the confidence of the signal observation and gives the discrimination power between the signal and background. The wide width is due to the jet-energy smearing discussed earlier. The other distinctive mass variable is $M_t^{rec} = M_{bbc}$, which reconstructs m_t for the signal and no structure for the background due to the incorrect jet combination. Similarly, $M_{\bar{t}}^{rec} \approx m_t$ for the signal but it spreads out for the background, as seen in Fig. 3(c). Those distributions motivate us to device more judicial kinematical cuts. Our basic kinematical cuts are listed in Table II based on these four reconstructed masses.

Additional cuts can be applied to further increase the signal-to-background ratio. We

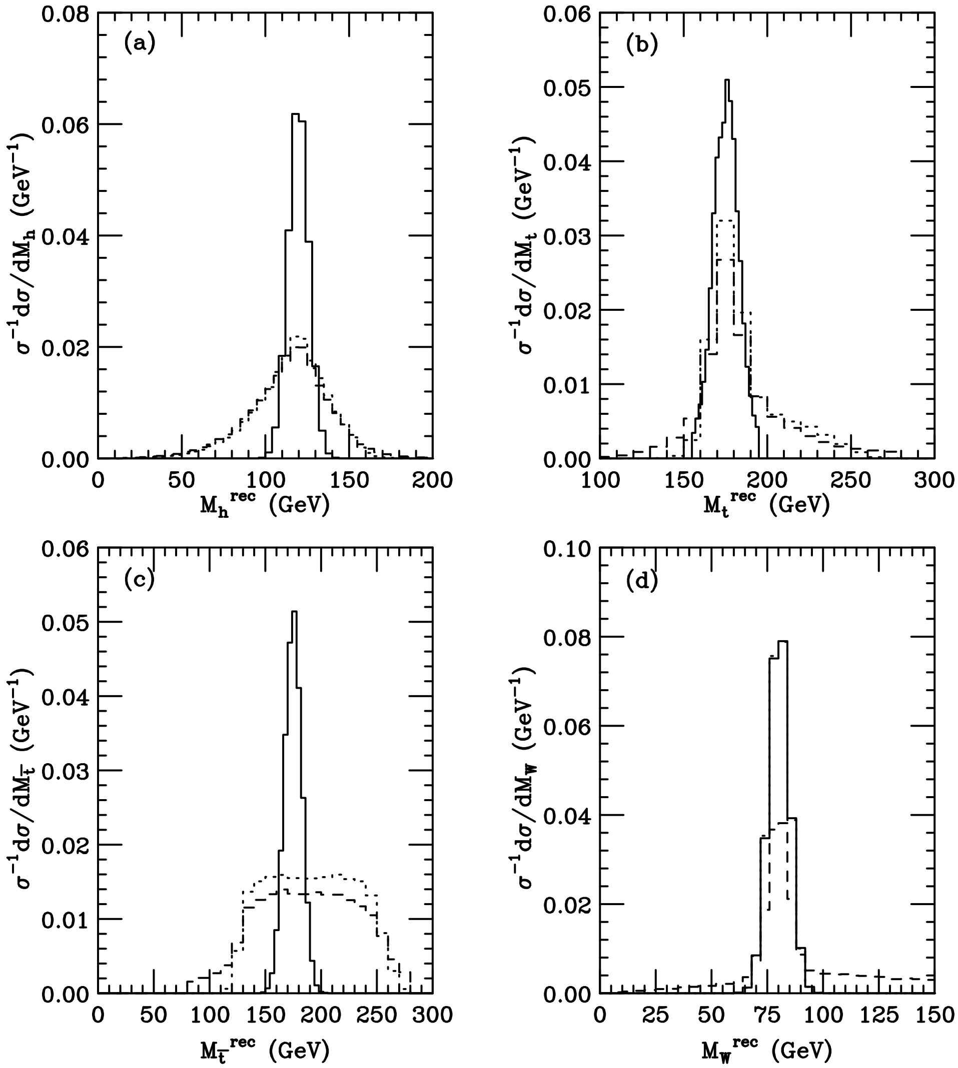

FIG. 3. Normalized distribution for the signal (solid), hadronic background (dashes) and leptonic background (dots) with respect to the reconstructed masses (a) M_h^{rec}, (b) M_t^{rec}, (c) $M_{\bar{t}}^{rec}$ and (d) M_W^{rec}, with $\sqrt{s} = 500$ GeV and $m_h = 120$ GeV.

first notice that the charm-jet energy from the top decay is monotonic in the top-rest frame as a result of a two-body decay

$$E_c^{rest} = \frac{m_t}{2}(1 - \frac{m_h^2}{m_t^2}), \tag{7}$$

which is about 50 GeV for $m_h = 120$ GeV. In contrast, the faked charm jet from W decay will have an energy more spread out. The normalized distributions are shown in Fig. 4. Figure 4(a) is the E_c distribution in the e^+e^-−lab frame which presents a nearly clear range due to the Lorentz boost of the top quark motion, where the sharp end-point in E_c is sensitive to m_h, that may provide an independent kinematical determination for m_h. Figure 4(b) shows the E_c distribution in the top-quark rest frame based on the $t \to b\bar{b}c$ reconstruction. We see that E_c is monotonic near 50 GeV modulus to the jet-energy resolution. This provides a good discriminator for the signal and background. In fact, the reconstructed Higgs boson

basic cuts	additional cuts
$110 < M_h^{rec} < 130$	$20 < E_c^{lab} < 130$
$160 < M_t^{rec},\ M_{\bar{t}}^{rec} < 190$	$40 < E_c^{rest} < 60$
$65 < M_W^{rec} < 95$	$E_b^{min} < 120,\ 80 < E_b^{max}$

TABLE II. The basic and additional kinematical cuts applied to our signal-to-background optimization (all values in GeV).

energy in the top-quark rest frame should be also monotonic $E_h^{rest} = \frac{m_t}{2}(1 + m_h^2/m_t^2)$, but it is correlated with E_c^{rest}. We also look at the two b-jets coming from h decay and examine the harder and softer ones of the two in energy, separately, as illustrated in Figs. 4(c) and 4(d). The optimal cuts are given in Table II. After applying the basic and additional cuts the signal-to-background ratio improves significantly, as summarized in the last two rows of Table I.

C. Sensitivity to the tch coupling

Given the efficient signal identification and substantial background suppression achieved in the previous section, we now estimate the sensitivity to the FCNC tch coupling from this reaction using Gaussian statistics, which is applicable for large signal event samples. We define the statistical significance by

$$\sigma = \frac{N_S}{\sqrt{N_S + N_B}}, \tag{8}$$

with N_S and N_B being the number of signal and background events. We note that $\sigma = 3$ (called 3σ) approximately corresponds to a 99% confidence level. Figure 5 presents the 3σ (2σ) sensitivity to the FCNC couplings by the solid (dashed) curve as a function of integrated luminosity for $\sqrt{s} = 500$ GeV and $m_h = 120$ GeV. Recall that at $\lambda_{ct} = 1$, the $t \to ch$ branching ratio is about 2.8×10^{-3}. Such an order of magnitude can be anticipated in models with tree-level FCNC couplings, and can be easily observed at a LC with an integrated luminosity of less than 40 fb^{-1}. As λ_{ct} varies, the branching ratio scales like $2.8 \times 10^{-3}\lambda_{ct}^2$. For 1-loop induced FCNC decays such as in SUSY models, the branching ratios can be about $10^{-5} - 5 \times 10^{-4}$, corresponding to λ_{ct} of $0.06 - 0.4$. A linear collider with 500 fb^{-1} integrated luminosity will begin to be sensitive to this range of the coupling of $\lambda_{ct} \approx 0.4$ (0.3) at a 3σ (2σ) level, but a higher luminosity will be needed to extend the coverage of the parameter space to a level about 0.2.

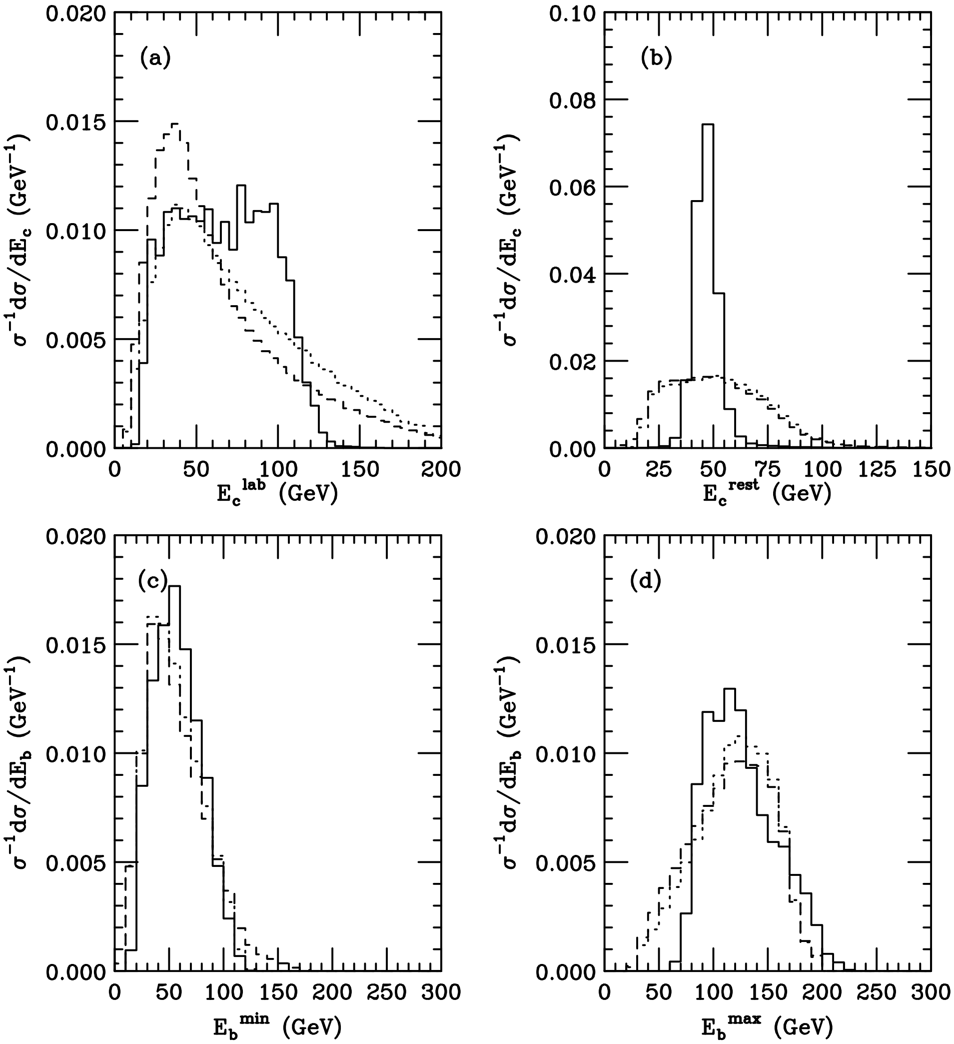

FIG. 4. Normalized distributions for signal (solid), hadronic background (dashes) and leptonic backgrounds (dots) with respect to (a) E_c^{lab}, (b) E_c^{rest}, (c) E_b^{min} and (d) E_b^{max}, with $\sqrt{s} = 500$ GeV and $m_h = 120$ GeV.

III. CONCLUSIONS

Models with a top-charm-Higgs coupling come in two categories: Those with a tree-level coupling and those with a coupling induced at one-loop. In the former case, such as the Model III two-Higgs doublet model, one expects λ_{ct} to be of $\mathcal{O}(1)$. If the Higgs is somewhat lighter than the top quark, then the $t \to ch$ decay will be detected within the first 40 fb^{-1} of running of a linear collider, as indicated in Fig. 5. In the latter case, such as supersymmetric models (in which we *know* that one of the Higgs bosons will be sufficiently light), the branching ratios can be in the range of 10^{-5} to a few times 10^{-4}. This corresponds to a λ_{ct} of $0.06 - 0.4$. A linear collider with 500 fb^{-1} integrated luminosity will begin to be sensitive to this range of the coupling at a 3σ level, and higher luminosity will be needed to substantially extend the coverage of the parameter space.

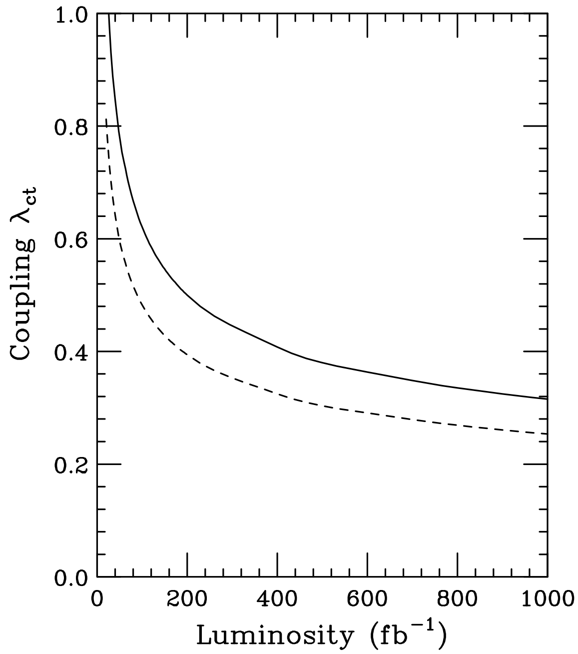

FIG. 5. 3σ sensitivity (solid) to the FCNC tch couplings at $\sqrt{s} = 500$ GeV for $m_h = 120$ GeV as a function of integrated luminosity. The dashed curve is for 2σ sensitivity.

Acknowledgments: The work of T.H. and J.J. was supported in part by a DOE grant No. DE-FG02-95ER40896 and in part by the Wisconsin Alumni Research Foundation. The work of M.S. was supported in part by an NSF grant No. PHY-9900657.

REFERENCES

[1] G. Eilam, J.L. Hewett and A. Soni, Phys. Rev. D**44**, 1473 (1991), erratum: Phys. Rev. D**59**, 039901 (1999).

[2] T. Han, R. D. Peccei, and X. Zhang, Nucl. Phys. B **454**, 527 (1995); T. Han, K. Whisnant, B.-L. Young, and X. Zhang, Phys. Rev. D **55**, 7241 (1997); Phys. Lett. B **385**, 311 (1996); M. Hosch, K. Whisnant, and B.-L. Young, Phys. Rev. D **56**, 5725 (1997); E. Malkawi and T. Tait, Phys. Rev. D **54**, 5758 (1996); T. Tait and C.P. Yuan, Phys. Rev. D **55**, 7300 (1997); T. Han, M. Hosch, K. Whisnant, B.-L. Young and X. Zhang, Phys. Rev. D **58**, 073008 (1998); F. del Aguila and J.A. Aguilar-Saavedra, Phys. Lett. B **462**, 310 (1999); F. del Aguila and J.A. Aguilar-Saavedra, Nucl. Phys. B **576**, 56 (2000).

[3] B. Mele, S. Petrarca and A. Soddu, Phys. Lett. B**435**, 401 (1998).

[4] T.P. Cheng and M. Sher, Phys. Rev. D**35**, 3484 (1987).

[5] G. Burdman, Phys. Rev. Lett. **83**, 2888 (1999).

[6] C.T. Hill, Phys. Lett. B **345**, 483(1995).

[7] H.-J. He and C.-P. Yuan, Phys. Rev. Lett. **83**, 28 (1999); H.-J. He, T. Tait and C.-P. Yuan, Phys. Rev. D**62**, 011702 (2000).

[8] A. Aranda and C. Carone, Phys. Lett. B**488**, 351 (2000).

[9] K. Higuchi and K. Yamamoto, Phys. Rev. D**62**, 073005 (2000).

[10] M. Sher and Y. Yuan, Phys. Rev. D**44**, 1461 (1991); D. Chang, W.S. Hou and W.Y. Keung, Phys. Rev. D**48**, 217 (1993); D. Atwood, L. Reina and A. Soni, Phys. Rev. Lett. **75**, 3800 (1995); Y. Grossman, Z. Ligeti and E. Nardi, Nucl. Phys. B**465**, 369 (1996); D. Atwood, L. Reina and A. Soni, Phys. Rev. D**54**, 3296 (1996); S.Y. Choi, C.S. Kim, Y.J. Kwon and S.H. Lee, Phys. Rev D**57**, 7023 (1998); G. Lopez Castro, R. Martinez and J.H. Munoz, Phys. Rev. D**58** 033003 (1998); D. Bowser-Chao, K. Cheung and W.Y. Keung, Phys. Rev. D**59**, 115006 (1999); K. Huitu, C.-D. Lu, P. Singer and D.-X. Zhang, Phys. Lett. B**445** 394 (1999); T.M. Aliev and M. Savci, Phys. Rev. D**60** 014005 (1999), J. Phys. G**26**, 997 (2000); S. Bergmann and Y. Nir, JHEP **9909**, 31 (1999); J. Diaz-Cruz and J.J. Toscano, Phys. Rev. D**62**, 116005 (2000); Z. Xiao, C.S. Li and K.T. Chao, Phys. Rev. D**62**, 094008 (2000); Phys. Rev. D**63**, 074005 (2001); S. Fajfer and P. Singer, Phys. Rev. D**62**, 117702 (2000).

[11] W.-S. Hou, Phys. Lett. B**296**, 179 (1992).

[12] W.-S. Hou and G.-L. Lin, Phys. Lett. B**379**, 261 (1996).

[13] W.-S. Hou, G.-L. Lin, C.-Y. Ma and C.-P. Yuan, Phys. Lett. B**409**, 344 (1997).

[14] S. Bar-Shalom, G. Eilam, A. Soni and J. Wudka, Phys. Rev. Lett. **79**, 1217 (1997); W.-S. Hou, G.-L. Lin and C.-Y. Ma, Phys. Rev. D**56**, 7434 (1997).

[15] J. Erler and P. Langacker, Eur. Phys. J. **C15**, 95 (2000).

[16] A.N. Okpara, in the proceedings of *36th Rencontres de Moriond on QCD and Hadronic Interactions, Les Arcs, France, 17-24 Mar 2001*, hep-ph/0105151.

[17] J. M. Yang and C.S. Li, Phys. Rev. D**49**, 3412 (1994); J. Guasch and J. Sola, Nucl. Phys. B**562**, 3 (1999); S. Bejar, J. Guasch and J. Sola, hep-ph/0101294.

[18] G. Eilam, A. Gemintern, T. Han, J.M. Yang and X. Zhang, hep-ph/0102037.

[19] C. Damerell and D. Jackson, in *Proceedings of the 1996 DPF/DPB Summer Study on New Directions for High Energy Physics.*

[20] J.A. Aguilar-Saavedra and G.C. Branco, Phys. Lett. B**495**, 347 (2000).